Journal of Computational Physics 238 (2013) 82–96

Contents lists available at SciVerse ScienceDirect

Journal of Computational Physics

journal homepage: www.elsevier.com/locate/jcp

Properties of the implicitly time-differenced equations of thermal radiation transport

Edward W. Larsen [a,*], Akansha Kumar [b], Jim E. Morel [b]

[a] Department of Nuclear Engineering and Radiological Sciences, University of Michigan, Ann Arbor, MI 48109-2104, USA
[b] Department of Nuclear Engineering, Texas A&M University, College Station, TX 77843, USA

ARTICLE INFO

Article history:
Received 26 June 2012
Received in revised form 6 November 2012
Accepted 14 November 2012
Available online 7 December 2012

Keywords:
Thermal radiation transport
Implicit time discretization

ABSTRACT

Numerical simulations of thermal radiation transport (TRT) use varying levels of implicitness to discretize the time variable t. The degree of implicitness generally depends on the strength of the coupling between the radiation and matter. In this paper we use a contraction mapping method to show that if all terms in the TRT equations except possibly the opacity are discretized implicitly, then for any $\Delta t > 0$, the time-discretized TRT equations (i) have a unique solution, which (ii) satisfies the maximum principle and (iii) preserves the equilibrium (thick) diffusion limit. No other available time-discretization of the TRT equations has all these desirable properties. Numerical results are included to illustrate the theoretical predictions.

1. Introduction

Thermal radiation transport (TRT) is the process of high-energy photons propagating in a physical system and interacting with the atoms within the system. When photons are absorbed by atoms, their energy is transferred to the atoms (the "material"), causing the material temperature to rise; when photons are emitted by atoms, their energy is lost from the material, causing the material temperature to fall. The value of the material temperature nonlinearly affects the rate at which the radiation interacts with the material. The TRT equations consist of an *equation of transfer* for the specific intensity of radiation, which is coupled to the *energy balance equation* for the material temperature [1,2]. The Planck function, opacities, and heat capacity in these equations all vary with the material temperature. TRT occurs in many areas of physics, such as the annealing of industrial glass, inertial confinement fusion experiments, and the modeling of supernovas.

Solutions of the TRT equations have properties that are not necessarily preserved in numerical simulations. One such property is the *maximum principle*, which states that if the initial and boundary conditions for a problem lie between two Planck functions, then the specific intensity will always lie between the two Planck functions for all points inside the system and all times after the initial time [3–7]. A second property is the *equilibrium diffusion limit*, which states that when a system becomes optically thick, its specific intensity is well-represented by a Planck function with a temperature $T(\boldsymbol{x}, t)$, which satisfies a nonlinear equilibrium diffusion equation [6–11]. In the present paper, we show that "implicit" time discretizations of the TRT equations, which have been used in deterministic simulations, preserve both the maximum principle and the equilibrium diffusion limit.

For problems in which the material and radiation are weakly coupled, conceptually simple explicit time differencing has been shown to be useful [12,13]. For more difficult problems in which the material and radiation are more tightly coupled, "weakly implicit" time discretizations – in which some but not all of the terms in the TRT equations are treated implicitly –

* Corresponding author. Tel.: +1 734 936 0124; fax: +1 734 763 4540.
E-mail addresses: edlarsen@umich.edu (E.W. Larsen), akansha@neo.tamu.edu (A. Kumar), morel@ne.tamu.edu (J.E. Morel).

0021-9991/$ - see front matter
http://dx.doi.org/10.1016/j.jcp.2012.11.034

become advantageous [14–17]. (The well-known weakly implicit IMC method is discussed in detail below.) Weakly implicit methods are more complicted and costly per time step than explicit methods. Both of these types of methods have the drawback that when the time step or the opacity becomes large, their solutions can become unphysical. Specifically, the numerical solutions may no longer satisfy the maximum principle, or the solution may become inaccurate for "diffusive" problems.

In this paper we consider "Almost Fully Implicit" (AFI) time discretizations of the TRT equations – in which all the terms in these equations, except possibly the opacity, are evaluated at the end of the time step. We show that for any $\Delta t > 0$, the AFI time-discretized RT equations have the following desirable properties: (i) they possess a unique solution, (ii) the solution satisfies the maximum principle, and (iii) the solution preserves the equilibrium diffusion limit. The analysis in this paper deals with time-discretization only; discretizations in the other independent variables (space, angle, and frequency) could possibly lead to unphysical solutions [18–22]. However, if unphysical results (non-existence of a solution, violations of the maximum principle, or inaccurate results for diffusive problems) are seen in simulations, the results in this paper guarantee that the fault does not lie with the AFI time discretization.

The maximum principle for TRT was originally derived in 1983 by Andreev, Kuzmanov, and Rachilov [3] for (i) the grey and continuous-frequency TRT equations, (ii) the grey thermal radiation diffusion equations, (iii) the grey thermal radiation diffusion equations with t discretized implicitly and x discretized in a standard way, and (iv) the grey TRT equations with t discretized implicitly, μ discretized by the discrete ordinates approximation, and x discretized using the "step" discretization. In the discrete results obtained by these authors, all quantities (including the opacities) are evaluated at the end of a time step, space-angle discretizations are chosen that are guaranteed to preserve the positivity of the continuous solution, and solutions of the resulting nonlinear equations are assumed to exist.

More recently, a modified equation analysis and numerical experimentation have shown that the 1-D radiation diffusion equations with semi-implicit time differencing can violate the maximum principle, but numerical results suggested that the same equations with implicit time differencing do not violate this principle [7]. Also, linearized stability analyses have recently shown that the explicitly and semi-implicitly time-discretized TRT equations have stability issues and can violate the maximum principle for large time steps [10,11], but again, numerical results suggest that the implicitly discretized equations are stable and do not violate the maximum principle [11].

The present paper extends these prior analyses to the AFI time-discretized 3-D radiative transfer equations, in which the opacities are evaluated at an arbitrary temperature during the time step, but all other quantities are evaluated at the end of the time step. No discretizations in space, direction-of-flight, or frequency are considered here. Our analysis, which treats the fully nonlinear TRT equations, is based on a standard contraction mapping argument from functional analysis [23].

In the sense that the present paper treats a specific TRT time-discretization scheme, it is similar to the 1971 paper by Fleck and Cummings [14], which introduced the so-called "Implicit Monte Carlo" time-discretization scheme for the same TRT equations. For each time step, the IMC method yields a linear transport equation with pseudoscattering, which can be simulated by a Monte Carlo method (and can be adapted to deterministic methods [16,21]). The IMC method has been used extensively for TRT simulations during the past 40 years. For sufficiently small Δt, it has been proved that IMC solutions will satisfy the maximum principle stated above [5]. However, the theoretical bound on Δt derived in [5] is several orders of magnitude smaller than time steps used in standard IMC simulations, and for realistic time steps, these simulations are often seen to violate the maximum principle.

We comment that the name *Implicit Monte Carlo* (IMC) given by Fleck and Cummings to their method in [14] is somewhat unfortunate, since only *some* of the terms in the TRT equations are treated implicitly. When *all* of the terms (except possibly the opacities) are treated implicitly, as they are in the present paper, the equations become nonlinear and do not have a known direct Monte Carlo interpretation. In the remainder of this paper, we continue to refer to the IMC method by its historical name, and we continue to refer to the time discretization method in this paper as Almost Fully Implicit (AFI). In doing this, we emphasize that the term "implicit" has a stricter meaning in this paper than it has in [14].

The remainder of this paper is organized as follows. In Section 2 the TRT equations are presented, along with several relevant features of these equations: equilibrium solutions, the maximum principle, the equilibrium diffusion limit, and the AFI time-discretized TRT equations. In Section 3 a contraction mapping argument shows that the AFI time-discretized TRT equations have a unique solution. In Section 4 this solution is shown to satisfy the same maximum principle as the solution of the analytic TRT equations. In Section 5, a formal asymptotic analysis demonstrates that for optically thick problems, the solution of the AFI TRT equations satisfies the implicitly-discretized equilibrium diffusion equation. (Thus, the time-discrete solution will be accurate if Δt adequately resolves the equilibrium diffusion solution.) In Section 6 we discuss the temperature at which the opacities can be evaluated; our theory indicates that there is considerable flexibility in this choice. Section 7 contains numerical results that illustrate the theory, and the paper concludes in Section 8 with a brief discussion.

2. The thermal radiation transport equations

Here we describe the TRT equations and some of their properties. We let $\boldsymbol{x} = (x, y, z)$ be the 3-D position variable for a specified physical system V, $\boldsymbol{\Omega} = (\Omega_x, \Omega_y, \Omega_z)$ be the direction of flight variable (with $\Omega_x^2 + \Omega_y^2 + \Omega_z^2 = 1$), ν = frequency (with $0 < \nu < \infty$), and t = time (with $t \geqslant 0$). The unknowns are:

$$I(\boldsymbol{x}, \boldsymbol{\Omega}, \nu, t) = \text{the specific intensity of radiation}, \tag{2.1a}$$

$$T(\boldsymbol{x}, t) = \text{the material temperature.} \tag{2.1b}$$

In the absence of material motion, scattering, heat conduction, and internal sources, the TRT equations for I and T consist of the *equation of transfer:*

$$\frac{1}{c}\frac{\partial I}{\partial t} + \boldsymbol{\Omega}\cdot\boldsymbol{\nabla} I = \sigma(B - I) \tag{2.2a}$$

and the *energy balance equation:*

$$\frac{\partial \mathcal{E}}{\partial t} = \iint \sigma(I - B)\, d\nu d\Omega, \tag{2.2b}$$

with the prescribed initial conditions

$$I(\boldsymbol{x}, \boldsymbol{\Omega}, \nu, 0) = I_i(\boldsymbol{x}, \boldsymbol{\Omega}, \nu), \tag{2.3a}$$

$$T(\boldsymbol{x}, 0) = T_i(\boldsymbol{x}), \tag{2.3b}$$

and the prescribed boundary condition

$$I(\boldsymbol{x}, \boldsymbol{\Omega}, \nu, t) = I_b(\boldsymbol{x}, \boldsymbol{\Omega}, \nu, t), \quad \boldsymbol{x} \in \partial V, \quad \boldsymbol{\Omega}\cdot\boldsymbol{n} < 0. \tag{2.4}$$

(These equations hold over all allowed ranges of the independent variables, unless specified otherwise. In Eq. (2.4), $\boldsymbol{n}$ is the unit outer normal vector on ∂V.) The prescribed nonnegative functions of T in the TRT equations are:

$$\sigma(\nu, T) = \text{opacity}, \tag{2.5a}$$

$$c_\nu(T) = \text{heat capacity}, \tag{2.5b}$$

$$\mathcal{E}(T) = \int_0^T c_\nu(T')dT' = \text{material energy density}, \tag{2.5c}$$

$$B(\nu, T) = \frac{2h\nu^3}{c^2}\left(e^{h\nu/kT} - 1\right)^{-1} = \text{Planck function}, \tag{2.5d}$$

and the specified constants in Eqs. (2.2) and (2.5) are c = the speed of light, h = Planck's constant, and k = Boltzmann's constant. The Planck function satisfies:

$$\iint B(\nu, T)\, d\nu d\Omega = acT^4, \tag{2.6a}$$

where

$$a = \frac{8\pi^3 k^4}{15h^3c^3} = \text{radiation constant.} \tag{2.6b}$$

Thus, the thermal radiation transport equations are linear in I, but nonlinear in T.

For $\sigma > 0$ (the situation of interest in this paper), the TRT equations have an infinite family of *equilibrium solutions*, which have no spatial, angular, or time dependence:

$$T(\boldsymbol{x}, t) = \mathcal{T} = (\text{any}) \text{ positive constant}, \tag{2.7a}$$

$$I(\boldsymbol{x}, \boldsymbol{\Omega}, \nu, t) = B(\nu, \mathcal{T}). \tag{2.7b}$$

From Eq. (2.5d), it can be shown that if T_L and T_U satisfy $T_L < T_U$, then for all ν:

$$B(\nu, T_L) < B(\nu, T_U).$$

The *maximum principle* can now be stated [3,4]. If (i) T_L and T_U are constant temperatures with $T_L < T_U$, (ii) the initial values of I and T satisfy:

$$B(\nu, T_L) \leqslant I_i(\boldsymbol{x}, \boldsymbol{\Omega}, \nu) \leqslant B(\nu, T_U), \tag{2.8a}$$

$$T_L \leqslant T_i(\boldsymbol{x}) \leqslant T_U, \tag{2.8b}$$

and (iii) the boundary values of I satisfy for all $t > 0$:

$$B(\nu, T_L) \leqslant I_b(\boldsymbol{x}, \boldsymbol{\Omega}, \nu, t) \leqslant B(\nu, T_U), \quad \boldsymbol{x} \in \partial V, \quad \boldsymbol{\Omega}\cdot\boldsymbol{n} < 0, \tag{2.9}$$

then the intensity I and material temperature T satisfy for all $t > 0$:

$$B(\nu, T_L) \leqslant I(\boldsymbol{x}, \boldsymbol{\Omega}, \nu, t) \leqslant B(\nu, T_U), \tag{2.10a}$$

$$T_L \leqslant T(\boldsymbol{x}, t) \leqslant T_U. \tag{2.10b}$$

As before, these equations hold over all allowed ranges of the independent variables.

Also, if the system V is optically thick, and the speed of light is fast compared to the time evolution of I, then the TRT Eqs. (2.2) can be scaled as:

$$\frac{\varepsilon}{c}\frac{\partial I}{\partial t} + \boldsymbol{\Omega} \cdot \boldsymbol{\nabla} I = \frac{\sigma}{\varepsilon}(B - I), \tag{2.11a}$$

$$\varepsilon \frac{\partial \mathcal{E}}{\partial t} = \iint \frac{\sigma}{\varepsilon}(I - B)\, d\nu d\Omega, \tag{2.11b}$$

with $0 < \varepsilon \ll 1$. Asymptotically expanding these equations for $\varepsilon \ll 1$, one obtains [8]:

$$I(\boldsymbol{x}, \boldsymbol{\Omega}, \nu, t) = B(\nu, T) + O(\varepsilon), \tag{2.12a}$$

where $T = T(\boldsymbol{x}, t)$ satisfies the *equilibrium diffusion equation*

$$\frac{\partial}{\partial t}\left[\mathcal{E}(T) + aT^4\right] = \boldsymbol{\nabla} \cdot \frac{ac}{3\sigma_R(T)} \boldsymbol{\nabla} T^4, \tag{2.12b}$$

and

$$\sigma_R(T) = \frac{\int \frac{\partial B}{\partial T}(\nu, T) d\nu}{\int \frac{1}{\sigma(\nu, T)} \frac{\partial B}{\partial T}(\nu, T) d\nu} = \text{Rosseland mean opacity}. \tag{2.12c}$$

We now consider an *AFI time-differenced* version of the TRT equations. Imposing a temporal grid $0 = t_0 < t_1 < t_2 < \cdots$, with $\Delta t_n = t_n - t_{n-1}$ = width of the nth time step, we time-discretize Eqs. (2.2) over the n^{th} time step as:

$$\frac{1}{c\Delta t_n}(I_n - I_{n-1}) + \boldsymbol{\Omega} \cdot \boldsymbol{\nabla} I_n = \sigma_*(B_n - I_n), \tag{2.13a}$$

$$\frac{1}{\Delta t_n}(\mathcal{E}_n - \mathcal{E}_{n-1}) = \iint \sigma_*(I_n - B_n) d\nu d\Omega. \tag{2.13b}$$

The initial conditions (2.3) give:

$$I_0(\boldsymbol{x}, \boldsymbol{\Omega}, \nu) = I_i(\boldsymbol{x}, \boldsymbol{\Omega}, \nu), \tag{2.14a}$$

$$T_0(\boldsymbol{x}) = T_i(\boldsymbol{x}), \tag{2.14b}$$

and the boundary condition (2.4) allows us to define:

$$I_n(\boldsymbol{x}, \boldsymbol{\Omega}, \nu) = \frac{1}{\Delta t_n}\int_{t_{n-1}}^{t_n} I_b(\boldsymbol{x}, \boldsymbol{\Omega}, \nu, t) dt \equiv I_{b,n}(\boldsymbol{x}, \boldsymbol{\Omega}, \nu), \quad \boldsymbol{x} \in \partial V, \quad \boldsymbol{\Omega} \cdot \boldsymbol{n} < 0. \tag{2.15}$$

In these equations we have defined the end-of-time-step quantities

$$I_n(\boldsymbol{x}, \boldsymbol{\Omega}, \nu) = I(\boldsymbol{x}, \boldsymbol{\Omega}, \nu, t_n), \tag{2.16a}$$

$$T_n(\boldsymbol{x}) = T(\boldsymbol{x}, t_n), \tag{2.16b}$$

$$B_n(\boldsymbol{x}, \nu) = B(\nu, T_n(\boldsymbol{x})), \tag{2.16c}$$

$$\mathcal{E}_n(\boldsymbol{x}) = \int_0^{T_n(\boldsymbol{x})} c_v(T') dT', \tag{2.16d}$$

and

$$\sigma_*(\boldsymbol{x}, \nu) = \sigma(\nu, T_*(\boldsymbol{x})), \tag{2.16e}$$

where $T_*(\boldsymbol{x})$ is any suitable estimate of the temperature *during* the nth time step. (For example, one could take $T_*(\boldsymbol{x}) = T_{n-1}(\boldsymbol{x})$. If instead $T_*(\boldsymbol{x}) = T_n(\boldsymbol{x})$, then the AFI method becomes fully implicit.) The flexibility in choosing $T_*(\boldsymbol{x})$ is discussed in detail later in Section 6.

In the remainder of this paper we consider the AFI time-discretized Eqs. (2.13)–(2.16) with no discretizations in space $\boldsymbol{x}$, angle $\boldsymbol{\Omega}$, or frequency ν. To implement these equations in a deterministic computer code, it is necessary to discretize $\boldsymbol{x}, \boldsymbol{\Omega}$, and ν, and then recursively solve the resulting system of nonlinear algebraic equations for each time step. If this is done, the analysis in this paper applies if the grids for $\boldsymbol{x}, \boldsymbol{\Omega}$, and ν are sufficiently fine and the convergence criterion is sufficiently small. Details of these extra discretizations and solution procedures have been treated elsewhere [18–22] and will not be discussed here.

3. Existence and uniqueness of a solution

To show that Eqs. (2.13)–(2.15) have a solution, we write Eq. (2.13) as

$$\left[\mathbf{\Omega}\cdot\nabla+\left(\sigma_*+\frac{1}{c\Delta t_n}\right)\right]I_n=\frac{1}{c\Delta t_n}I_{n-1}+\sigma_*B_n, \tag{3.1a}$$

$$\frac{1}{\Delta t_n}\mathcal{E}(T_n)+\iint\sigma_*(\nu)B(\nu,T_n)d\nu d\Omega=\frac{1}{\Delta t_n}\mathcal{E}(T_{n-1})+\iint\sigma_*(\nu)I_n d\nu d\Omega. \tag{3.1b}$$

These equations are to be solved with the initial and boundary conditions (2.14) and (2.15).

First, we note that for any positive constant $\mathcal{T}$, Eq. (3.1) have the equilibrium solution

$$T_n(\boldsymbol{x})=\mathcal{T}, \tag{3.2a}$$

$$I_n(\boldsymbol{x},\mathbf{\Omega},\nu)=B(\nu,\mathcal{T}). \tag{3.2b}$$

Thus, the implicit TRT equations preserve the equilibrium solutions of the TRT equations.

To proceed, we define (see Fig. 1):

$$\ell(\boldsymbol{x},\mathbf{\Omega})\equiv\text{the distance from }\boldsymbol{x}\text{ to }\partial V\text{ in the direction }-\mathbf{\Omega}, \tag{3.3a}$$

$$\boldsymbol{x}_b=\boldsymbol{x}-\ell(\boldsymbol{x},\mathbf{\Omega})\mathbf{\Omega}. \tag{3.3b}$$

Then solving the first-order partial differential Eq. (3.1a) with the boundary condition (2.15), we obtain

$$I_n(\boldsymbol{x},\mathbf{\Omega},\nu)=\mathcal{K}_nI_{b,n}(\boldsymbol{x},\mathbf{\Omega},\nu)+\mathcal{L}_n\left(\frac{1}{c\Delta t_n}I_{n-1}+\sigma_*B_n\right)(\boldsymbol{x},\mathbf{\Omega},\nu), \tag{3.4}$$

where the linear operators $\mathcal{K}_n$ and $\mathcal{L}_n$ are defined by

$$\mathcal{K}_nf(\boldsymbol{x},\mathbf{\Omega},\nu)=f(\boldsymbol{x}_b,\mathbf{\Omega},\nu)e^{-\int_0^{\ell(\boldsymbol{x},\mathbf{\Omega})}\left[\sigma_*(\boldsymbol{x}-s'\mathbf{\Omega},\nu)+\frac{1}{c\Delta t_n}\right]ds'}, \tag{3.5a}$$

$$\mathcal{L}_ng(\boldsymbol{x},\mathbf{\Omega},\nu)=\int_0^{\ell(\boldsymbol{x},\mathbf{\Omega})}g(\boldsymbol{x}-s\mathbf{\Omega},\mathbf{\Omega},\nu)e^{-\int_0^s\left[\sigma_*(\boldsymbol{x}-s'\mathbf{\Omega},\nu)+\frac{1}{c\Delta t_n}\right]ds'}ds. \tag{3.5b}$$

For any two functions $f(\boldsymbol{x},\mathbf{\Omega},\nu)$ and $g(\boldsymbol{x},\mathbf{\Omega},\nu)$, which are identically zero for $\boldsymbol{x}$ outside V, the following identity holds:

$$\begin{aligned}\int\iint g(\boldsymbol{x},\mathbf{\Omega},\nu)\mathcal{L}_nf(\boldsymbol{x},\mathbf{\Omega},\nu)dVd\Omega d\nu&=\int\iint g(\boldsymbol{x},\mathbf{\Omega},\nu)\left\{\int_{s=0}^{\infty}\int_V\delta(\boldsymbol{x}'-\boldsymbol{x}+s\mathbf{\Omega})f(\boldsymbol{x}',\mathbf{\Omega},\nu)\times e^{-\int_0^s\left[\sigma_*(\boldsymbol{x}'+(s-s')\mathbf{\Omega},\nu)+\frac{1}{c\Delta t_n}\right]ds'}dV'ds\right\}dVd\Omega d\nu\\&=\int\iint\left\{\int_{s=0}^{\infty}\int_V\delta(\boldsymbol{x}-\boldsymbol{x}'+s\mathbf{\Omega})g(\boldsymbol{x}',\mathbf{\Omega},\nu)e^{-\int_0^s\left[\sigma_*(\boldsymbol{x}+(s-s')\mathbf{\Omega},\nu)+\frac{1}{c\Delta t_n}\right]ds'}dV'ds\right\}\times f(\boldsymbol{x},\mathbf{\Omega},\nu)dVd\Omega d\nu\\&=\int\iint\left\{\int_{s=0}^{\infty}\int_V\delta(\boldsymbol{x}-\boldsymbol{x}'+s\mathbf{\Omega})g(\boldsymbol{x}',\mathbf{\Omega},\nu)e^{-\int_0^s\left[\sigma_*(\boldsymbol{x}+s''\mathbf{\Omega},\nu)+\frac{1}{c\Delta t_n}\right]ds''}dV'ds\right\}\times f(\boldsymbol{x},\mathbf{\Omega},\nu)dVd\Omega d\nu\\&=\int\iint\left[\mathcal{L}_n^*g(\boldsymbol{x},\mathbf{\Omega},\nu)\right]f(\boldsymbol{x},\mathbf{\Omega},\nu)dVd\Omega d\nu.\end{aligned}$$

Thus the adjoint operator $\mathcal{L}_n^*$ is defined by

$$\mathcal{L}_n^*g(\boldsymbol{x},\mathbf{\Omega},\nu)=\int_0^{\ell(\boldsymbol{x},-\mathbf{\Omega})}g(\boldsymbol{x}+s\mathbf{\Omega},\mathbf{\Omega},\nu)e^{-\int_0^s\left[\sigma_*(\boldsymbol{x}+s'\mathbf{\Omega},\nu)+\frac{1}{c\Delta t_n}\right]ds'}ds. \tag{3.6}$$

In particular, the function $\mathcal{L}_n^*\sigma_*$ satisfies

$$\mathcal{L}_n^*\sigma_*(\boldsymbol{x},\mathbf{\Omega},\nu)=\int_0^{\ell(\boldsymbol{x},-\mathbf{\Omega})}\sigma_*(\boldsymbol{x}+s\mathbf{\Omega},\mathbf{\Omega},\nu)e^{-\int_0^s\left[\sigma_*(\boldsymbol{x}+s'\mathbf{\Omega},\nu)+\frac{1}{c\Delta t_n}\right]ds'}ds\geqslant 0,$$

and also, this nonnegative function has the upper bound

$$0\leqslant\mathcal{L}_n^*\sigma_*(\boldsymbol{x},\mathbf{\Omega},\nu)\leqslant\int_0^{\ell(\boldsymbol{x},-\mathbf{\Omega})}\sigma_*(\boldsymbol{x}+s\mathbf{\Omega},\mathbf{\Omega},\nu)e^{-\int_0^s\sigma_*(\boldsymbol{x}+s'\mathbf{\Omega},\nu)ds'}ds=1-e^{-\int_0^{\ell(\boldsymbol{x},-\mathbf{\Omega})}\sigma_*(\boldsymbol{x}+s\mathbf{\Omega},\nu)ds}. \tag{3.7}$$

These inequalities are used later.

Returning to Eq. (3.1b), we define the nonlinear function of T:

$$g_{n,\boldsymbol{x}}(T)\equiv\frac{1}{\Delta t_n}\mathcal{E}(T)+4\pi\int\sigma_*(\boldsymbol{x},\nu)B(\nu,T)d\nu, \tag{3.8a}$$

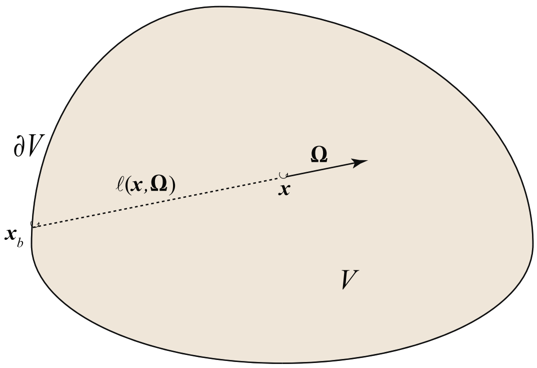

Fig. 1. The distance-to-boundary function $\ell(x, \boldsymbol{\Omega})$.

which satisfies

$$\frac{dg_{n,\boldsymbol{x}}}{dT}(T) = \frac{1}{\Delta t_n} c_v(T) + 4\pi \int \sigma_*(\boldsymbol{x}, \nu) \frac{\partial B}{\partial T}(\nu, T) d\nu > 0. \tag{3.8b}$$

Since $g_{n,\boldsymbol{x}}(T)$ is a monotonically increasing function of T, it has a unique, monotonically increasing inverse function $g^{-1}_{n,\boldsymbol{x}}(T)$, satisfying

$$U = g_{n,\boldsymbol{x}}(T) \quad \text{if and only if} \quad g^{-1}_{n,\boldsymbol{x}}(U) = T. \tag{3.9}$$

The left side of Eq. (3.1b) is now $g_{n,\boldsymbol{x}}(T_n)$, so Eq. (3.1b) can be written

$$T_n = g^{-1}_{n,\boldsymbol{x}}\left[\frac{1}{\Delta t_n}\mathcal{E}(T_{n-1}) + \iint \sigma_*(\nu) I_n d\nu d\Omega\right]. \tag{3.10}$$

Eqs. (3.1) and (2.4) have now been expressed in the equivalent form of Eqs. (3.4) and (3.10). We rewrite the latter two equations as

$$I_n(\boldsymbol{x}, \boldsymbol{\Omega}, \nu) = \mathcal{K}_n I_{b,n} + \mathcal{L}_n\left(\frac{1}{c\Delta t_n} I_{n-1} + \sigma_* B_n\right), \tag{3.11a}$$

$$\Phi_n(\boldsymbol{x}) = \iint \sigma_*(\nu) I_n d\nu d\Omega, \tag{3.11b}$$

$$T_n(\boldsymbol{x}) = g^{-1}_{n,\boldsymbol{x}}\left[\frac{1}{\Delta t_n}\mathcal{E}(T_{n-1}) + \Phi_n\right], \tag{3.11c}$$

and we reiterate that for any positive constant temperature $\mathcal{T}$, these equations have the equilibrium solution:

$$B(\nu, \mathcal{T}) = \mathcal{K}_n B(\nu, \mathcal{T}) + \mathcal{L}_n\left(\frac{1}{c\Delta t_n} B(\nu, \mathcal{T}) + \sigma_* B(\nu, \mathcal{T})\right), \tag{3.12a}$$

$$\Phi(\mathcal{T}) = \iint \sigma_*(\nu) B(\nu, \mathcal{T}) d\nu d\Omega, \tag{3.12b}$$

$$\mathcal{T} = g^{-1}_{n,\boldsymbol{x}}\left[\frac{1}{\Delta t_n}\mathcal{E}(\mathcal{T}) + \Phi(\mathcal{T})\right]. \tag{3.12c}$$

To prove the existence of a solution of Eq. (3.11) for the first time step ($n = 1$), let us consider the sequence $I^{(k)}(\boldsymbol{x}, \boldsymbol{\Omega}, \nu), \Phi^{(k)}(\boldsymbol{x})$, and $T^{(k)}(\boldsymbol{x})$, defined for $k = 0$ by

$$I^{(0)} = I_0, \tag{3.13a}$$

$$\Phi^{(0)} = \iint \sigma_*(\nu) I^{(0)} d\nu d\Omega, \tag{3.13b}$$

$$T^{(0)} = T_0, \tag{3.13c}$$

and for $k \geqslant 1$ by

$$I^{(k)} = \mathcal{K}_1 I_{b,1} + \mathcal{L}_1\left(\frac{1}{c\Delta t_1} I_0 + \sigma_* B(\nu, T^{(k-1)})\right), \tag{3.14a}$$

$$\Phi^{(k)} = \iint \sigma_*(\nu) I^{(k)} d\nu d\Omega, \tag{3.14b}$$

$$T^{(k)} = g_{1,\boldsymbol{x}}^{-1}\left[\frac{1}{\Delta t_1}\mathcal{E}(T_0) + \Phi^{(k)}\right]. \tag{3.14c}$$

(This sequence is defined by the familiar source-iteration procedure, with the initial estimate defined in terms of the intensity and temperature at the beginning of the time step.)

For any $k \geqslant 1$, Eqs. (3.14a) and (3.14b) give

$$\Phi^{(k+1)} = \iint \sigma_*\left[\mathcal{K}_1 I_{b,1} + \mathcal{L}_1\left(\frac{1}{c\Delta t_1} I_0 + \sigma_* B(\nu, T^{(k)})\right)\right] d\nu d\Omega, \tag{3.15a}$$

and Eq. (3.14c) gives

$$g_{n,\boldsymbol{x}}(T^{(k)}) = \frac{1}{\Delta t_1}\mathcal{E}(T_0) + \Phi^{(k)}. \tag{3.15b}$$

Eqs. (3.15) implicitly define a nonlinear mapping from $\Phi^{(k)}(\boldsymbol{x})$ to $\Phi^{(k+1)}(\boldsymbol{x})$:

$$\Phi^{(k+1)}(\boldsymbol{x}) = F_1[\Phi^{(k)}(\boldsymbol{x})]. \tag{3.16}$$

We now prove that the nonlinear operator F_1 is a *contraction mapping* [23], i.e. a constant $\rho < 1$ exists such that for any two functions $\Phi_1(\boldsymbol{x})$ and $\Phi_2(\boldsymbol{x})$ defined on V,

$$\int_V |F_1[\Phi_2] - F_1[\Phi_1]| dV \leqslant \rho \int_V |\Phi_2 - \Phi_1| dV. \tag{3.17}$$

To accomplish this, we make use of the identity

$$F_1[\Phi_2] - F_1[\Phi_1] = \int_0^1 \frac{d}{dt} F_1[\Phi_1 + t(\Phi_2 - \Phi_1)]\, dt = \int_0^1 F_1'[\Phi_1 + t(\Phi_2 - \Phi_1)](\Phi_2 - \Phi_1)\, dt = \int_0^1 F_1'[\Phi(t)]\Delta\Phi\, dt, \tag{3.18a}$$

where

$$\Phi(t) = \Phi_1 + t(\Phi_2 - \Phi_1), \tag{3.18b}$$
$$\Delta\Phi = \Phi_2 - \Phi_1. \tag{3.18c}$$

To construct the linear operators $F_1'[\Phi(t)]$, we note that $F_1[\Phi]$ is defined implicitly by Eq. (3.15):

$$F_1[\Phi] = \iint \sigma_*\left[\mathcal{K}_1 I_{b,1} + \mathcal{L}_1\left(\frac{1}{c\Delta t_1} I_0 + \sigma_* B(\nu, T)\right)\right] d\nu d\Omega, \tag{3.19a}$$

$$g_{1,\boldsymbol{x}}(T) = \frac{1}{\Delta t_1}\mathcal{E}(T_0) + \Phi. \tag{3.19b}$$

For any function $\Delta\Phi(\boldsymbol{x}), F_1[\Phi + \varepsilon\Delta\Phi]$ and $\Delta T(\boldsymbol{x})$ are defined by

$$F_1[\Phi + \varepsilon\Delta\Phi] = \iint \sigma_*\left[\mathcal{K}_1 I_{b,1} + \mathcal{L}_1\left(\frac{1}{c\Delta t_1} I_0 + \sigma_* B(\nu, T + \varepsilon\Delta T)\right)\right] d\nu d\Omega, \tag{3.20a}$$

$$g_{1,\boldsymbol{x}}(T + \varepsilon\Delta T) = \frac{1}{\Delta t_1}\mathcal{E}(T_0) + \Phi + \varepsilon\Delta\Phi. \tag{3.20b}$$

Expanding Eq. (3.20a) for $\varepsilon \approx 0$ and using Eqs. (3.19a), we get

$$\begin{aligned} F_1[\Phi + \varepsilon\Delta\Phi] &= \iint \sigma_*\left[\mathcal{K}_1 I_{b,1} + \mathcal{L}_1\left(\frac{1}{c\Delta t_1} I_0 + \sigma_* B(\nu, T) + \sigma_* \frac{\partial B}{\partial T}(\nu, T)\,\varepsilon\Delta T\right) + O(\varepsilon^2)\right] d\nu d\Omega \\ &= F_1[\Phi] + \varepsilon \iint \sigma_* \mathcal{L}_1 \sigma_* \frac{\partial B}{\partial T}(\nu, T)\,\Delta T d\nu d\Omega + O(\varepsilon^2). \end{aligned} \tag{3.21a}$$

Also, Eqs. (3.20b) and (3.19b) give

$$g_{1,\boldsymbol{x}}(T + \varepsilon\Delta T) = g_{1,\boldsymbol{x}}(T) + \varepsilon\Delta\Phi. \tag{3.21b}$$

Rewriting the previous two equations, we obtain

$$\frac{1}{\varepsilon}(F_1[\Phi + \varepsilon\Delta\Phi] - F_1[\Phi]) = \iint \sigma_* \mathcal{L}_1 \sigma_* \frac{\partial B}{\partial T}(\nu, T)\,\Delta T d\nu d\Omega + O(\varepsilon). \frac{1}{\varepsilon}\left(g_{1,\boldsymbol{x}}(T + \varepsilon\Delta T) - g_{1,\boldsymbol{x}}(T)\right) = \Delta\Phi.$$

Letting $\varepsilon \to 0$, we get

$$F_1'[\Phi]\Delta\Phi = \iint \sigma_* \mathcal{L}_1 \sigma_* \frac{\partial B}{\partial T}(\nu, T)\,\Delta T d\nu d\Omega, \quad g_{1,\boldsymbol{x}}'(T)\Delta T = \Delta\Phi.$$

Using the second of these equations to eliminate ΔT from the first, we obtain

$$F_1'[\Phi]\Delta\Phi = \iint \sigma_* \mathcal{L}_1 \sigma_* \frac{\partial B}{\partial T}(\nu, T)\,\frac{\Delta\Phi}{g_{1,\boldsymbol{x}}'(T)} d\nu d\Omega, \tag{3.22}$$

where $T = T(\Phi)$ is defined by Eq. (3.19b).

Since $\mathcal{L}, \sigma_*, \partial B/\partial T$, and $g_{1,\boldsymbol{x}}'(T)$ are positive, we get [using Eq. (3.8b)] the following inequality:

$$\begin{aligned}\int_V |F_1'[\Phi]\Delta\Phi|\,dV &\leqslant \int \iint \sigma_* \mathcal{L}_1 \sigma_* \frac{\partial B}{\partial T}\frac{|\Delta\Phi|}{g_{1,\boldsymbol{x}}'(T)} d\Omega d\nu dV = \int \iint (\mathcal{L}_1^* \sigma_*)\sigma_* \frac{\partial B}{\partial T}\frac{|\Delta\Phi|}{g_{1,\boldsymbol{x}}'(T)} d\Omega d\nu dV \\ &= \int_V \left[\frac{\iint (\mathcal{L}_1^* \sigma_*)\sigma_* \frac{\partial B}{\partial T} d\Omega d\nu}{\frac{1}{\Delta t_1} c_\nu(T) + \iint \sigma_* \frac{\partial B}{\partial T} d\Omega d\nu}\right] |\Delta\Phi| dV. \end{aligned} \tag{3.23a}$$

From Eq. (3.6) and the positivity of $c_\nu(T)$, we have

$$\max_{\boldsymbol{x}\in V}\left[\frac{\iint (\mathcal{L}_1^* \sigma_*)\sigma_* \frac{\partial B}{\partial T} d\Omega d\nu}{\frac{1}{\Delta t_1} c_\nu(T) + \iint \sigma_* \frac{\partial B}{\partial T} d\Omega d\nu}\right] \equiv \rho < 1. \tag{3.23b}$$

Thus, Eqs. (3.23) imply that using the L_1 norm:

$$||\Delta\Phi|| = \int_V |\Delta\Phi(\boldsymbol{x})|\,dV,$$

the linear operator $F_1'[\Phi]$ has a norm bounded less than unity:

$$||F_1'[\Phi]|| = \sup_{\Delta\Phi}\frac{||F_1'[\Phi]\Delta\Phi||}{||\Delta\Phi||} \leqslant \rho < 1. \tag{3.24}$$

Eqs. (3.18) and (3.24) immediately give for any Φ_1 and Φ_2:

$$||F_1[\Phi_2] - F_1[\Phi_1]|| \leqslant \int_0^1 ||F_1'[\Phi_1 + t(\Phi_2 - \Phi_1)](\Phi_2 - \Phi_1)||\,dt \leqslant \int_0^1 \rho\,||(\Phi_2 - \Phi_1)||\,dt = \rho\,||(\Phi_2 - \Phi_1)||. \tag{3.25}$$

This result, with the bound $\rho < 1$, establishes that F_1 is a *contraction mapping* [23].

Returning to the sequence $\Phi^{(k)}$ defined by Eq. (3.14), we have

$$\Phi^{(k+1)} - \Phi^{(k)} = F_1[\Phi^{(k)}] - F_1[\Phi^{(k-1)}],$$

so, by Eq. (3.25),

$$||\Phi^{(k+1)} - \Phi^{(k)}|| = ||F_1[\Phi^{(k)}] - F_1[\Phi^{(k-1)}]|| \leqslant \rho\,||\Phi^{(k)} - \Phi^{(k-1)}||. \tag{3.26}$$

Therefore, the sequence of functions $\{\Phi^{(k)}(\boldsymbol{x})\}$ is a Cauchy sequence in L_1 [23]; hence the sequence converges, and we name the limiting result $\Phi_1(\boldsymbol{x})$:

$$\lim_{k\to\infty}\Phi^{(k)}(\boldsymbol{x}) \equiv \Phi_1(\boldsymbol{x}). \tag{3.27}$$

Clearly, $\Phi_1(\boldsymbol{x})$ satisfies Eq. (3.16):

$$\Phi_1 = F_1[\Phi_1]. \tag{3.28}$$

Also, $\Phi_1(\boldsymbol{x})$ is unique; if another solution Ψ_1 of Eq. (3.28) were to exist, then

$$||\Phi_1 - \Psi_1|| = F_1[\Phi_1] - F_1[\Psi_1]|| \leqslant \rho\,||\Phi_1 - \Psi_1||,$$

so $||\Phi_1 - \Psi_1||$ = 0.

This establishes the unique existence of a solution I_1, Φ_1, and T_1 of Eq. (3.11) for the first time step ($n = 1$). The same analysis can be repeated for the next time step ($n = 2$), and for the time step after that, etc. A simple induction argument (described in detail in the next section) then shows that Eqs. (3.11) have a unique solution for all time steps $n \geqslant 1$.

4. The maximum principle

To show that the solution (whose existence and uniqueness is shown in Section 3) satisfies the maximum principle, we now assume that the initial conditions (2.14) satisfy

$$B(\nu,T_L) \leqslant I_0(\boldsymbol{x},\boldsymbol{\Omega},\nu) \leqslant B(\nu,T_U), \tag{4.1a}$$
$$T_L \leqslant T_0(\boldsymbol{x}) \leqslant T_U, \tag{4.1b}$$

and the boundary condition (2.15) satisfies for all $n \geqslant 1$

$$B(\nu,T_L) \leqslant I_{b,n}(\boldsymbol{x},\boldsymbol{\Omega},\nu) \leqslant B(\nu,T_U), \quad \boldsymbol{x} \in \partial V, \ \ \boldsymbol{\Omega}\cdot\boldsymbol{n} < 0. \tag{4.2}$$

We wish to show that for all $n \geqslant 1$

$$B(\nu,T_L) \leqslant I_n(\boldsymbol{x},\boldsymbol{\Omega},\nu) \leqslant B(\nu,T_U), \tag{4.3a}$$
$$T_L \leqslant T_n(\boldsymbol{x}) \leqslant T_U. \tag{4.3b}$$

To do this, we consider again the sequence $I^{(k)}, \Phi^{(k)}$, and $T^{(k)}$ defined by Eqs. (3.13) and (3.14), for the first ($n = 1$) time step. By Eqs. (3.13) and (4.1), $I^{(0)}$ and $T^{(0)}$ satisfy

$$B(\nu,T_L) \leqslant I^{(0)}(\boldsymbol{x},\boldsymbol{\Omega},\nu) \leqslant B(\nu,T_U), \tag{4.4a}$$
$$T_L \leqslant T^{(0)}(\boldsymbol{x}) \leqslant T_U. \tag{4.4b}$$

Eqs. (3.14a), (4.1), and (4.2) give

$$I^{(1)} = \mathcal{K}_1 I_{b,1} + \mathcal{L}_1\left(\frac{1}{c\Delta t_1}I_0 + \sigma_* B(\nu,T^{(0)})\right) \leqslant \mathcal{K}_1 B(\nu,T_U) + \mathcal{L}_1\left(\frac{1}{c\Delta t_1}B(\nu,T_U) + \sigma_* B(\nu,T_U)\right) = B(\nu,T_U),$$

and similarly

$$I^{(1)} \geqslant \mathcal{K}_1 B(\nu,T_L) + \mathcal{L}_1\left(\frac{1}{c\Delta t_1}B(\nu,T_L) + \sigma_* B(\nu,T_L)\right) = B(\nu,T_L).$$

Thus, we have:

$$B(\nu,T_L) \leqslant I^{(1)}(\boldsymbol{x},\boldsymbol{\Omega},\nu) \leqslant B(\nu,T_U). \tag{4.5a}$$

This result and Eqs. (3.14b) and (3.14c) imply

$$\begin{aligned} T^{(1)}(\boldsymbol{x}) &= g_{1,\boldsymbol{x}}^{-1}\left[\frac{1}{\Delta t_1}\mathcal{E}(T_0(\boldsymbol{x})) + \iint \sigma_*(\nu) I^{(1)}(\boldsymbol{x},\boldsymbol{\Omega},\nu)d\nu d\Omega\right] \leqslant g_{1,\boldsymbol{x}}^{-1}\left[\frac{1}{\Delta t_1}\mathcal{E}(T_U) + \iint \sigma_*(\nu)B(\nu,T_U)d\nu d\Omega\right] = g_{1,\boldsymbol{x}}^{-1}[g_{1,\boldsymbol{x}}(T_U)] \\ &= T_U, \end{aligned}$$

and similarly,

$$T^{(1)}(\boldsymbol{x}) \geqslant g_{1,\boldsymbol{x}}^{-1}\left[\frac{1}{\Delta t_1}\mathcal{E}(T_L) + \iint \sigma_*(\nu)B(\nu,T_L)d\nu d\Omega\right] = g_{1,\boldsymbol{x}}^{-1}[g_{1,\boldsymbol{x}}(T_L)] = T_L.$$

Thus, we also have

$$T_L \leqslant T^{(1)}(\boldsymbol{x}) \leqslant T_U. \tag{4.5b}$$

Using the bounds (4.5), one can use the same approach to prove that $I^{(2)}$ and $T^{(2)}$ also satisfy (4.5); and this analysis can be repeated for as many successive time steps as desired. Thus, by induction, we obtain for all $k \geqslant 1$

$$B(\nu,T_L) \leqslant I^{(k)}(\boldsymbol{x},\boldsymbol{\Omega},\nu) \leqslant B(\nu,T_U), \tag{4.6a}$$
$$T_L \leqslant T^{(k)}(\boldsymbol{x}) \leqslant T_U. \tag{4.6b}$$

Letting $k \to \infty$, we obtain the result that Eqs. (4.3) hold for the first time step ($n = 1$).

The same analysis can be repeated for the next time step ($n = 2$), and the time step after that, and so on. Thus, by induction, Eqs. (4.3) hold for all time steps $n \geqslant 1$.

This establishes that the unique solution I_n, Φ_n, and T_n of Eqs. (3.11) satisfies the maximum principle, for all time steps and any choice of $\Delta t_n > 0$.

5. The equilibrium diffusion limit

The AFI time-discretized TRT Eqs. (2.13) with the diffusive asymptotic scaling (2.11) are:

$$\frac{\varepsilon}{c\Delta t_n}(I_n - I_{n-1}) + \boldsymbol{\Omega}\cdot\nabla I_n = \frac{\sigma_*}{\varepsilon}(B_n - I_n), \tag{5.1a}$$
$$\frac{\varepsilon}{\Delta t_n}(\mathcal{E}_n - \mathcal{E}_{n-1}) = \iint \frac{\sigma_*}{\varepsilon}(I_n - B_n)d\nu d\Omega, \tag{5.1b}$$

with $\varepsilon \ll 1$. We will show that I_n asymptotically satisfies a robust AFI time discretization of the equilibrium diffusion equation defined by Eqs. (2.12).

To do this, we write Eq. (5.1a) as

$$\left(I + \frac{\varepsilon}{\sigma_*}\boldsymbol{\Omega}\cdot\boldsymbol{\nabla} + \frac{\varepsilon^2}{\sigma_* c\Delta t_n}\right)I_n = \left(B_n + \frac{\varepsilon^2}{\sigma_* c\Delta t_n}I_{n-1}\right),$$

where I is the identity operator. Formally solving this equation for I_n, we get:

$$\begin{aligned} I_n &= \left[I + \left(\frac{\varepsilon}{\sigma_*}\boldsymbol{\Omega}\cdot\boldsymbol{\nabla} + \frac{\varepsilon^2}{\sigma_* c\Delta t_n}\right)\right]^{-1}\left(B_n + \frac{\varepsilon^2}{\sigma_* c\Delta t_n}I_{n-1}\right) = \sum_{n=0}^{\infty}\left(-\frac{\varepsilon}{\sigma_*}\boldsymbol{\Omega}\cdot\boldsymbol{\nabla} - \frac{\varepsilon^2}{\sigma_* c\Delta t_n}\right)^n\left(B_n + \frac{\varepsilon^2}{\sigma_* c\Delta t_n}I_{n-1}\right) \\ &= B_n - \frac{\varepsilon}{\sigma_*}\boldsymbol{\Omega}\cdot\boldsymbol{\nabla}B_n + \frac{\varepsilon^2}{\sigma_*}\left(\frac{1}{c\Delta t_n}(I_{n-1} - B_n) + \boldsymbol{\Omega}\cdot\boldsymbol{\nabla}\frac{1}{\sigma_*}\boldsymbol{\Omega}\cdot\boldsymbol{\nabla}B_n\right) + O(\varepsilon^3). \end{aligned}$$

Using $I_{n-1} = B_{n-1} + O(\varepsilon)$ and rearranging, we obtain

$$\sigma_*(I_n - B_n) = -\varepsilon\boldsymbol{\Omega}\cdot\nabla B_n + \varepsilon^2\left(\frac{1}{c\Delta t_n}(B_{n-1} - B_n) + \boldsymbol{\Omega}\cdot\boldsymbol{\nabla}\frac{1}{\sigma_*}\boldsymbol{\Omega}\cdot\boldsymbol{\nabla}B_n\right) + O(\varepsilon^3).$$

Operating by $\int(\cdot)d\Omega$, we get

$$\int \sigma_*(I_n - B_n)d\Omega = \varepsilon^2\left[\frac{4\pi}{c\Delta t_n}(B_{n-1} - B_n) + \boldsymbol{\nabla}\cdot\frac{4\pi}{3\sigma_*}\boldsymbol{\nabla}B_n\right] + O(\varepsilon^3),$$

and then operating by $\int_0^\infty(\cdot)d\nu$, we get, using Eq. (2.6a),

$$\iint \sigma_*(I_n - B_n)d\Omega d\nu = \varepsilon^2\left[\frac{a}{\Delta t_n}\left(T_{n-1}^4 - T_n^4\right) + \boldsymbol{\nabla}\cdot\frac{1}{3}\int\frac{4\pi}{\sigma_*}\boldsymbol{\nabla}B_n d\nu\right] + O(\varepsilon^3). \tag{5.2}$$

However, Eq. (2.6a) also gives

$$\int\frac{4\pi}{\sigma_*}\boldsymbol{\nabla}B_n d\nu = \left(\int\frac{1}{\sigma_*}\frac{\partial B_n}{\partial T}d\nu\right)4\pi\boldsymbol{\nabla}T_n(\boldsymbol{x}) = \left(\frac{\int\frac{1}{\sigma_*}\frac{\partial B_n}{\partial T}d\nu}{\int\frac{\partial B_n}{\partial T}d\nu}\right)\left(4acT_n^3\right)\boldsymbol{\nabla}T_n(\boldsymbol{x}) = \frac{ac}{\sigma_{R,*}}\boldsymbol{\nabla}T_n^4,$$

where

$$\sigma_{R,*} = \left(\frac{\int\frac{1}{\sigma_*}\frac{\partial B_n}{\partial T}d\nu}{\int\frac{\partial B_n}{\partial T}d\nu}\right)^{-1} = \text{Rosseland mean opacity}. \tag{5.3}$$

Thus, Eq. (5.2) can be written

$$\iint \sigma_*(I_n - B_n)d\Omega d\nu = \varepsilon^2\left[\frac{a}{\Delta t_n}\left(T_{n-1}^4 - T_n^4\right) + \boldsymbol{\nabla}\cdot\frac{ac}{3\sigma_{R,*}}\boldsymbol{\nabla}T_n^4\right] + O(\varepsilon^3).$$

Introducing this result into Eq. (5.1b) and using $\mathcal{E}_n = \mathcal{E}(T_n)$, we obtain with $O(\varepsilon^2)$ error:

$$\frac{1}{\Delta t_n}\left[\left(\mathcal{E}(T_n) + aT_n^4\right) - \left(\mathcal{E}(T_{n-1}) + aT_{n-1}^4\right)\right] = \boldsymbol{\nabla}\cdot\frac{ac}{3\sigma_{R,*}}\boldsymbol{\nabla}T_n^4. \tag{5.4}$$

This is a well-behaved, AFI time discretization of the equilibrium diffusion equation. In the Rosseland mean opacity, $\sigma(\nu, T)$ is evaluated at $T = T_*$, while $\partial B/\partial T(\nu, T)$ is evaluated at the end-of-time-step temperature $T = T_n$. When $\boldsymbol{x}$ is discretized in Eq. (5.4), the resulting fully discrete equation will yield accurate results if the temporal and spatial grids are chosen to resolve the equilibrium diffusion problem.

Remark 1. It has long been known that a discrete version of the TRT equations does not necessarily lead to an accurate discrete version of the equilibrium diffusion problem when the diffusive scaling of Eqs. (2.11) is applied to the discrete equations [6,7,9–11,16–21,24]. (In particular, the time and spatial discretization methods, and of course the choice of grids, have a major role to play in whether this desirable result occurs.) The preceding analysis shows that if a discrete version of Eq. (5.1) behaves poorly in the limit $\varepsilon \to 0$, it is not the fault of the implicit time differencing scheme.

6. Definition of T_*

One final theoretical detail remains to be discussed: the choice of $T_*(\boldsymbol{x})$ in Eq. (2.16e).

The existence, uniqueness, maximum principle, and equilibrium diffusion limit results derived in the preceding sections have been shown to hold for any $T_*(\boldsymbol{x})$. Thus, the choice of $T_*(\boldsymbol{x})$ has no effect on the existence of a solution, or on the solution's ability to satisfy the maximum principle, or the equilibrium diffusion limit. The only effect that the choice of $T_*(\boldsymbol{x})$ has on the solution is *accuracy*. This suggests that $T_*(\boldsymbol{x})$ could be chosen to make the solution as accurate as possible.

The simplest choice of $T_*(\boldsymbol{x})$ for the nth time step is to define this quantity explicitly:

$$T_*(\boldsymbol{x}) = T_{n-1}(\boldsymbol{x}).$$

However, since the opacities generally evolve during the time step, a more accurate result should be obtained by choosing $T_*(\boldsymbol{x})$ neither explicitly ($T_* = T_{n-1}$) nor implicitly ($T_* = T_n$), but rather at some intermediate value between $T_{n-1}(\boldsymbol{x})$ and $T_n(\boldsymbol{x})$. For instance, Wollaber [24] obtained good results for $\sigma = \gamma/T^3$ by setting

$$\overline{\sigma} = \frac{1}{\Delta t}\int_{T_{n-1}}^{T_n} \frac{\gamma}{T^3}\, dT = \frac{\gamma}{T_*^3} = \sigma(T_*),$$

which yields

$$T_*(\boldsymbol{x}) = \left(\frac{2T_{n-1}^2(\boldsymbol{x})T_n^2(\boldsymbol{x})}{T_{n-1}(\boldsymbol{x}) + T_n(\boldsymbol{x})}\right)^{1/3}.$$

Of course, defining T_* in terms of T_n requires a good estimate of T_n, and obtaining this requires extra computational work. [For instance, one could (i) estimate T_n using an inexpensive deterministic method, (ii) use this estimate to define T_*, and (iii) proceed with the calculation of I_n and T_n; this was done in [24]. Alternatively, one could (i) use $T_* = T_{n-1}$ to obtain an estimate of I_n and T_n, (ii) use the resulting estimate of T_n to redefine T_*, and (iii) solve the resulting equations again to obtain new estimates of I_n and T_n.]

It is clear that however T_* is defined, the resulting method will be remain first-order in time:

$$\text{Error at time } t = C(t)\Delta t,$$

where $C(t) = O(1)$ for $t = O(1)$. Nonetheless, by defining T_* judiciously, $C(t)$ could likely be reduced, with minimal cost, from its value obtained by setting $T_* = T_n$. The question of defining T_* will not be discussed further here.

7. Numerical results

To illustrate the theory developed above, we consider numerical simulations of a grey 1-D Marshak wave problem. The physical system is a slab 0.02 cm thick, with

$$\sigma(T) = \frac{300}{T^3} \quad (\mathrm{cm}^{-1}), \tag{7.1a}$$

$$\mathcal{E}(\mathrm{T}) = \rho \mathrm{C_v T} = 0.3\mathrm{T} \quad (\mathrm{jks/cm^3}), \tag{7.1b}$$

where T is defined in units of keV, and 1 jerk = 10^9 joules. At the initial time $t = 0$, the slab is in equilibrium, with

$$T(x,0) = T_0 = 0.01 \quad (\mathrm{KeV}), \tag{7.2a}$$

$$I(x,\mu,0) = \frac{acT_0^4}{4\pi} = \text{Planckian at temperature } T_0. \tag{7.2b}$$

For $t > 0$, an incident Planckian flux at temperature 1.0 keV is imposed on the left boundary ($x = 0$), and the right boundary ($x = 0.02$ cm) is made reflecting. At the initial temperature (10.0 eV) the problem domain is 6×10^6 mean-free-paths thick; at the final temperature (1.0 keV) it becomes 6.0 mean-free-paths thick. Thus, the problem is initially diffusive and becomes non-diffusive only in the relatively hot region through which the wavefront has passed. (The narrow wavefront is a transition region in which an initially diffusive region becomes non-diffusive.)

This problem was simulated using (i) the AFI method with the opacity evaluated at the end-of-time-step temperature (resulting in the *fully-implicit* method), and (ii) a *weakly implicit* (WI) time discretization method described in [20]. The WI scheme consists of a single iteration each time step of an approximate form of Newton's method for the fully-implicit equations. This approximate Newton's method is completely characterized for a time step from t_{n-1} to t_n by linearization about T_{n-1} while neglecting contributions to the Jacobian from the opacity.

A uniform spatial grid of 50 cells (Δx = 0.0004 cm) was used for the spatial variable, with the standard S_8 Gauss–Legendre quadrature set used for the angular variable. Descriptions of the spatial and angular discretizations, together with the iteration strategy used to solve the discrete equations, are given in [20]. To implement the AFI method, the approximate Newton method described above was simply iterated to convergence each time step.

In Fig. 2, the solutions obtained with $\Delta t = 5.75 \times 10^{-13}$ s are plotted (i) at the end of each of the first five time steps, and (ii) at the fixed times $t_1 = 2.3 \times 10^{-11}$ s, $t_2 = 5.75 \times 10^{-11}$ s, $t_3 = 1.15 \times 10^{-10}$ s, and $t_4 = 1.72 \times 10^{-10}$ s. The AFI and WI solutions are very similar at all the plotted times, and there is no sign of an instability or a violation of the maximum principle.

In Fig. 3, the solution calculated with the (larger) time step $\Delta t = 1.15 \times 10^{-12}$ s is also plotted at the end of the first five time steps and at the fixed times t_1, t_2, t_3, and t_4. The AFI solution exhibits no unphysical behavior; close examination shows that the AFI solutions at times t_1, t_2, t_3, and t_4 are nearly identical in Figs. 2 and 3 (see Fig. 5).

The WI solution violates the maximum principle during the first three time steps but then ‘‘settles down’’ and resembles a standard Marshak wave for later times. However, the early instability in the WI solution causes an overly advanced wavefront at late times (Also, note the change in vertical scale from Figs. 2 and 3).

In Fig. 4, the solutions with the (even larger) time step $\Delta t = 2.3 \times 10^{-12}$ s are plotted at the end of the first five time steps and at times t_1, t_2, t_3, and t_4. The unphysical behavior of the WI solution is now accentuated; the maximum principle is vio-

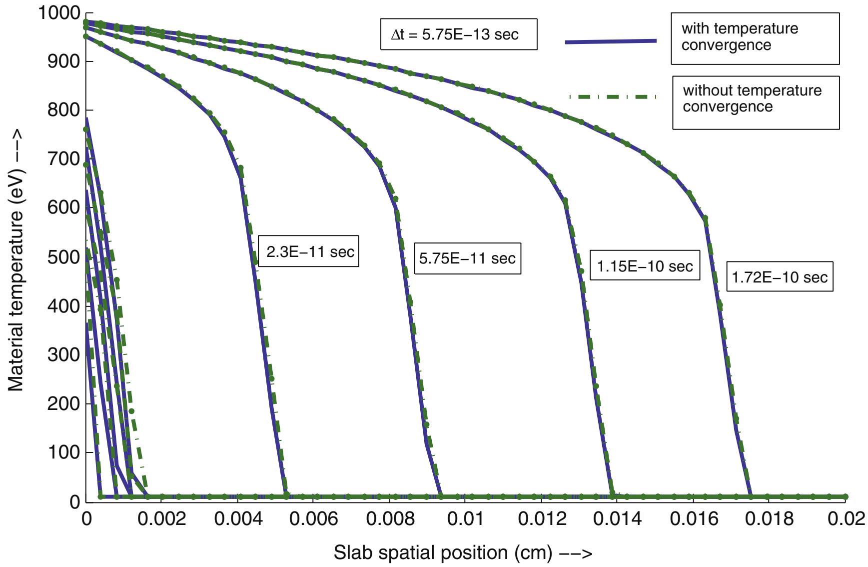

Fig. 2. Marshak wave problem with $\Delta t = 5 \times 10^{-13}$ s.

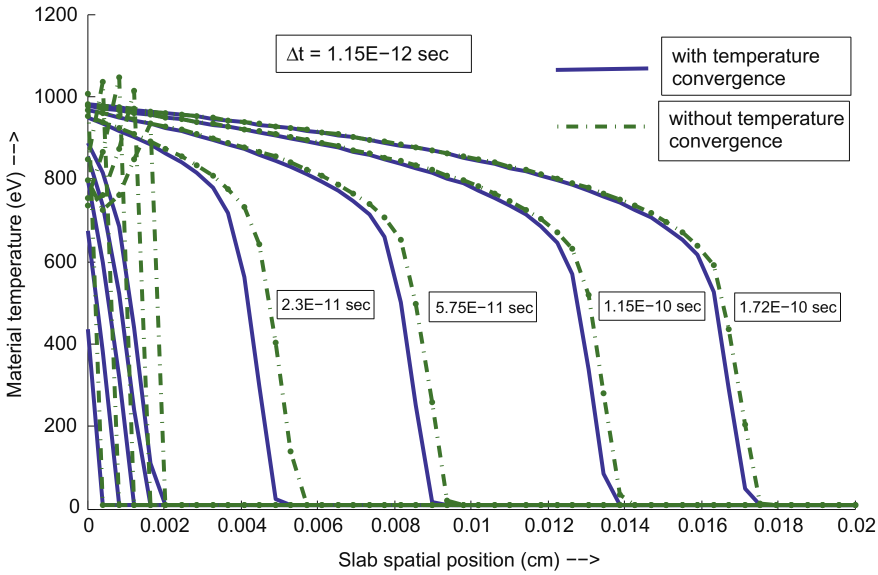

Fig. 3. Marshak wave problem with $\Delta t = 10^{-12}$ s.

lated to a significantly greater extent, and for many more time steps. The WI solution does "settle down" for much later times than in Fig. 3, but its wavefront is then much further advanced.

In Fig. 5, the AFI solutions from Figs. 2–4 are plotted at the fixed times t_1, t_2, t_3, and t_4. This plot shows that the AFI solutions satisfy the maximum principle for all three values of Δt and experience almost no loss of accuracy as Δt increases.

All the previous results were obtained with the opacity treated implicitly (evaluated at the converged, end-of-timestep temperature). To test the theory in this paper, we also ran simulations with the opacity treated explicitly (evaluated at the beginning-of-timestep temperature). We found that – consistent with the theory – the solutions still preserved the maximum principle. However, these "explicit-opacity" solutions were slightly less accurate than the "implicit-opacity" solutions for large Δt.

To illustrate, Fig. 6 compares the implicit-opacity solution with explicit-opacity solutions at the times t_1, t_2, t_3, and t_4, generated with the same three values of Δt used in Fig. 5. (The implicit-opacity solution is identical to the solution "with temperature convergence" plotted in Fig. 4.) Also, the explicit-opacity solution obtained with $\Delta_t = 5.75 \times 10^{-13}$ s (the coarsest

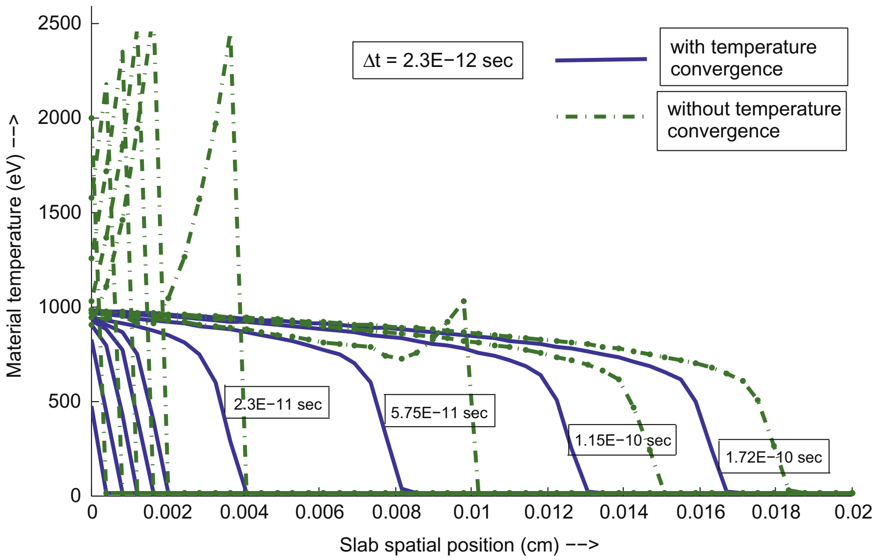

Fig. 4. Marshak wave problem with $\Delta t = 2 \times 10^{-12}$ s.

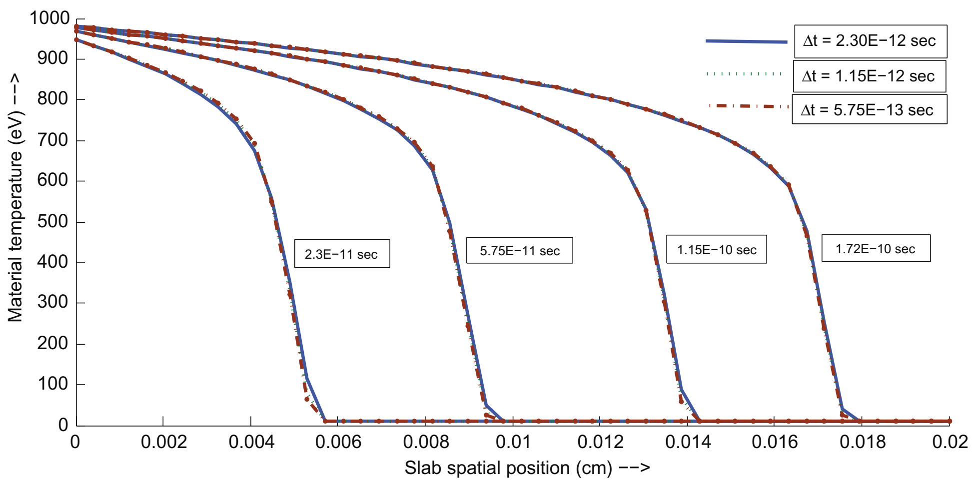

Fig. 5. Implicit solutions at fixed times for varying Δt.

Δt) is plotted for the first five time steps. Fig. 6 confirms that the solutions obtained with explicit opacities preserve the maximum principle but lag slightly behind the solutions obtained with implicit opacities. (This can be explained physically: the explicit opacities are slightly “colder,” making the system more optically thick. Hence, the thermal wave propagates into the system more slowly.) As Δt decreases, the explicit-opacity solutions are seen to limit to the implicit-opacity solution.

The numerical results presented above are consistent with the maximum principle (stability) and diffusion limit (accuracy) theories developed in this paper. These theories do not predict that the numerical AFI solution will remain highly accurate for larger Δt; also, the theories have nothing to say about the accuracy of the solutions for larger values of Δx. However, the theories do predict that the AFI time discretization of the TRT equations will preserve the maximum principle and the diffusion approximation, and these properties of the continuous thermal radiation transport equations should be preserved if the spatial and angular discretizations of the TRT equations are adequate.

8. Discussion

The results in this paper show that if the thermal radiation transport (TRT) equations are time-discretized by evaluating all quantities except possibly the opacities at the end-of-timestep temperature $T_n(x)$, then for any $\Delta t > 0$, (i) a unique solution of the time-discretized equations exists, (ii) this solution satisfies the maximum principle, and (iii) the solution pre-

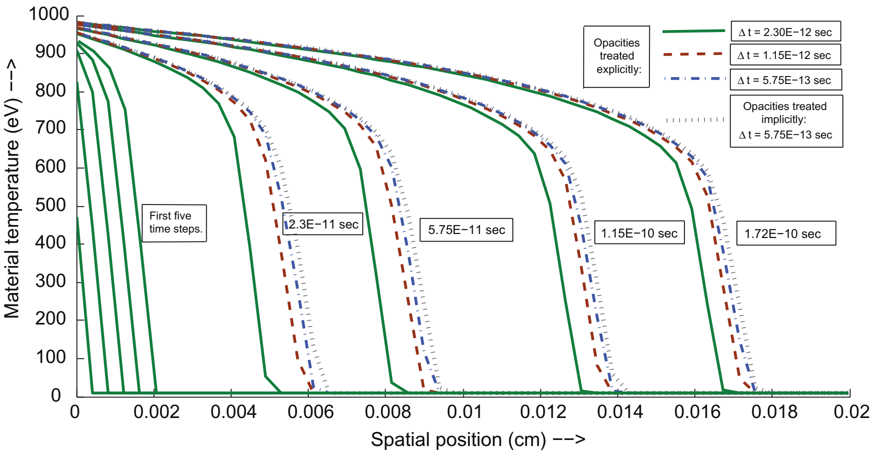

Fig. 6. AFI solutions with explicit opacities at fixed times for varying Δt.

serves the equilibrium diffusion limit. This provides a theoretical explanation to experimental observations that for larger time steps, implicit time discretizations make TRT simulations (i) preserve the maximum principle and (ii) generally more accurate [7].

The theory presented in this paper does not say whether the favorable results just cited will hold when the spatial, angular, and frequency variables are discretized. (In fact, the issues associated with spatial discretizations of particle transport problems for diffusive systems are nontrivial and have been extensively studied [18–22].) However, if the spatial, angular, and frequency variables are discretized using proper methods, and if the grids for these variables are adequate, then the results of this paper should apply.

The AFI time discretization of the TRT equations requires that certain nonlinearities – in particular, the Planck function and the heat capacity – be evaluated at the end-of-time-step temperature. This requires an iterative procedure, which is currently not a realistic option for Monte Carlo (IMC) simulations. However, it is a straightforward option for deterministic methods, which require iterations anyway to converge the "pseudoscattering" source [7,16,21]. Therefore, the theory in this paper is more relevant and applicable to deterministic simulations than to Monte Carlo simulations.

Nonetheless, the results in this paper suggest that a possible way to improve the stability and accuracy of the IMC method is to estimate the end-of-timestep temperature $\hat{T}_n(x)$ by an inexpensive deterministic method, and then run the IMC calculation with the normalized Planck function and heat capacity evaluated at $\hat{T}_n(x)$, rather than $T_{n-1}(x)$. Wollaber experienced some success with this approach [24].

The analysis in Sections 3 and 4 of this paper relies on standard monotonicity and contraction mapping arguments. No linearization is required, and no restriction is placed on the problem being close to an infinite-medium equilibrium solution. The existence of a unique solution of the implicitly-discretized TRT equations is proved by a *constructive procedure*: a sequence of iterates is defined and is shown (by a contraction mapping argument) to converge to the desired result. This sequence is defined as the familiar *source iteration* procedure (called *lambda iteration* in the astrophysics community). Lambda iterations are the basis of deterministic numerical iterations for the RT equations. Unfortunately, for optically thick problems lambda iterations converge slowly; accelerating these iterations has been the topic of much prior research [18–21]. Fortunately for the theory in this paper, proving the existence of a solution requires only that the lambda iterations converge; it does not matter how slowly they converge.

Acknowledgments

The work by A. Kumar and J. Morel was supported in part by Lawrence Livermore National Laboratory under contract C12-00768.

References

[1] G.C. Pomraning, The Equations of Radiation Hydrodynamics, Pergamon Press, Oxford (1973). Reprinted by Dover (2005).
[2] D. Mihalas, B.W. Mihalas, Foundations of Radiation Hydrodynamics, Oxford University Press, New York, 1984.
[3] E.S. Andreev, M.Yu. Kuzmanov, E.B. Rachilov, U.S.S.R. Comput. Math. Math. Phys. 23 (1983) 104.
[4] B. Mercier, Application of accretive operators theory to radiative transfer equations, SIAM J. Math. Anal. 18 (1987) 393.
[5] E.W. Larsen, B. Mercier, Analysis of a Monte Carlo method for nonlinear radiative transfer, J. Comput. Phys. 71 (1987) 50.
[6] J.D. Densmore, E.W. Larsen, Asymptotic equilibrium diffusion analysis of time-dependent Monte Carlo methods for Grey radiative transfer, J. Comput. Phys. 199 (2004) 175.

[7] D.A. Knoll, R.B. Lowrie, J.E. Morel, Numerical analysis of time integration errors for nonequilibrium radiation diffusion, J. Comput. Phys. 226 (2007) 1332.
[8] E.W. Larsen, G.C. Pomraning, V.C. Badham, Asymptotic analysis of radiative transfer problems, J. Quant. Spectrosc. Rad. Transfer 29 (1983) 285.
[9] A.B. Wollaber, E.W. Larsen, A linear stability analysis for nonlinear, 1-D, Gray implicit Monte Carlo calculations, in: Proceedings of 2009 International Conference on Advances in Mathematics, Computational Methods, and Reactor Physics, May 3–7, 2009, Saratoga Springs, New York, CD-ROM, American Nuclear Society, 2009.
[10] A.B. Wollaber, E.W. Larsen, A linear stability analysis for nonlinear, Grey, thermal radiative transfer problems, J. Comput. Phys. 230 (2011) 1528.
[11] J.E. Morel, R. McClarren, Stability of explicit radiation-material coupling in radiative transfer calculations, J. Quant. Spectrosc. Rad. Transfer 112 (2011) 1518.
[12] S. Mazumder, A new numerical procedure for coupling radiation in participating media with other modes of heat transfer, J. Heat Transfer 127 (2005) 1037.
[13] R.W. Hogan, D.K. Gartling, Solution strategies for coupled conduction/radiation problems, Commun. Num. Methods Eng. 24 (2007) 523.
[14] J.A. Fleck Jr., J.D. Cummings, An implicit Monte Carlo scheme for calculating time and frequency dependent nonlinear radiation transport, J. Comput. Phys. 8 (1971) 313.
[15] J.A. Fleck Jr., E.H. Canfield, A random walk procedure for improving the computational efficiency of the implicit Monte Carlo method for nonlinear radiation transport, J. Comput. Phys. 54 (1984) 508.
[16] R.E. Alcouffe, B.A. Clark, E.W. Larsen, The diffusion-synthetic acceleration of transport iterations, with application to a radiation hydrodynamics problem, in: J.U. Brackbill, B.I. Cohen (Eds.), Multiple Time Scales, Academic Press, Orlando, 1985.
[17] A. Klar, C. Schmeiser, Numerical passage from radiative heat transfer to nonlinear diffusion models, Math. Models Methods Appl. Sci. 11 (2001) 749.
[18] E.W. Larsen, J.E. Morel, W.F. Miller Jr., Asymptotic solutions of numerical transport problems in optically thick, diffusive regimes, J. Comput. Phys. 69 (1987) 283.
[19] E.W. Larsen, J.E. Morel, Asymptotic solutions of numerical transport problems in optically thick, diffusive regimes II, J. Comput. Phys. 83 (1989) 212.
[20] J.E. Morel, T.A. Wareing, K. Smith, A linear-discontinuous spatial differencing scheme for SN radiative transfer calculations, J. Comput. Phys. 128 (1996) 445.
[21] M.L. Adams, P.F. Nowak, Asymptotic analysis of a computational method for time- and frequency-dependent radiative transfer, J. Comput. Phys. 146 (1998) 366.
[22] E.W. Larsen, J.E. Morel, Advances in discrete-ordinates methodology, in: Y.Y. Azmy, E. Sartori (Eds.), Nuclear Computational Science: A Century in Review, Springer, Germany, Dordrecht, 2010, pp. 1–84.
[23] G. Bachman, L. Narici, Functional Analysis, Academic Press, New York, 1966.
[24] A.B. Wollaber, Advanced Monte Carlo Methods for Thermal Radiation Transport, Ph.D. Dissertation, University of Michigan, 2008.